S©MR ISSN 1813-3304

СИБИРСКИЕ ЭЛЕКТРОННЫЕ
МАТЕМАТИЧЕСКИЕ ИЗВЕСТИЯ

Siberian Electronic Mathematical Reports
http://semr.math.nsc.ru

*Том 15, стр. 1735–1742 (2018)* УДК 519.63
DOI 10.33048/semi.2018.15.143 MSC 65N30

# SENSITIVITY OF THE PRESSURE DECLINE CURVE DURING THE HYDRAULIC FRACTURING TO POROELASTIC EFFECTS

E.V. LGOTINA, A.N. BAYKIN, S.V. GOLOVIN, A.M. KRIVTSOV

Abstract. Computer simulators of hydraulic fracturing rely on known physical properties of the reservoir, in particular, the leak-off coefficient and the confining in situ stress. This information can be obtained from the solution of the inverse problem by analyzing of the pressure decline curve (PDC) in pump-in/shut-in tests. The goal of the present work is to demonstrate that poroelastic effect can have significant influence on the behavior of the PDC and, hence, to results of its analysis.

For computer simulations we use the mathematical model of the hydraulic fracture in poroelastic medium developed in [6]. We investigate the dependence of the PDC on the closure stress and of the rock permeability. It is shown that classical methods for interpretation of PDC can lead to a significant error, in particular, in estimation of the minimal in situ confining stress.

**Keywords:** hydraulic fracture, mathematical modeling, pressure decline curve, poroelastic effects.

## 1. Introduction

Hydraulic fracturing is a key technology for stimulation of low-permeable oil and gas reservoirs. The fracture is created due to the injection of highly pressurized fluid in a certain part of the wellbore. The resulting fracture with the characteristic length up to first hundreds meters, acts as a highly permeable channel for the inflow of oil or gas from the reservoir into the well.

The geometry of the fracture and its productivity can be estimated by the mathematical modeling. The model must reflect the coupled physical processes:

---

Lgotina, E.V., Baykin, A.N., Golovin, S.V., Krivtsov, A.M., Sensitivity of the pressure decline curve during the hydraulic fracturing to poroelastic effects.



This work was financially supported by the Ministry of Science and Higher Education of the Russian Federation in the framework of the Federal Program “Research and Development in the Priority Areas of Development of the Russian Scientific and Technical Complex for 2014-2020”, Activity 1.2., Subsidy Agreement в,– 14.575.21.0146 of 26.09.2017. Unique project identifier: RFMEFI57517X0146.

*Received October, 28, 2018, published December, 26, 2018.*

flow of viscous fluid within the fracture, an elastic reaction of the walls, a leak-off into the reservoir, energy losses due the material failure at the fracture tip, etc.

Numerical modeling of the hydraulic fracture propagation relies on the relevant information about physical properties of the reservoir and its stress-strain state. These parameters are usually determined using various kinds of dynamic well tests including shut-in/pump-in (mini-frac) tests where a pressure decline curve is to be interpreted by a solution of the inverse problem. The existing methods of analyzing mini-frac tests enable estimating several of important parameters and indicators such as a fracture closure pressure, a fluid efficiency, a closure stress, a leak-off coefficient, friction losses, etc. Virtually, all modern hydraulic fracturing simulators include special tools for interpreting the pressure decline curve. Models of hydraulic fracturing used in the engineering practice are based on the assumption that the medium is formed of horizontal uniform and isotropic elastic rock layers. The fluid leak-off from the fracture into the medium is approximated via Carter formula [4] whereas the effects of the pore pressure on the fracture opening are not taken into account.

Nevertheless, the results of [6, 2] indicate that under the plain strain condition the influence of pore fluid pressure on the rock deformation, as well as the reverse effect on fluid filtration, may significantly affect the fracture opening development. The earlier study [3] of the pressure field data in mini-frac tests also confirms the significance of poroelastic effects. Thus, in order to conduct dynamic well tests properly one should use a more sophisticated poroelastic model for pressure curve interpretation.

In current paper we investigate the possibility of mini-frac pressure curves interpretation, based on the direct simulation of a hydraulic fracture that takes poroelastic effects into account. The sensitivity of the pressure time history and fracture geometry to the reservoir permeability and closure stress is analyzed.

The characteristic points on the pressure decline curve for shut-in stage are identified: the time of the injection stop and the time of the fracture closure. The obtained results serve as a basis for a further development of the more accurate methods for a mini-frac data interpretation.

## 2. Mathematical formulation of the problem

The mathematical model presented in this paper was proposed and analyzed in authors' earlier works [1, 6, 2]. Here for consistency, we give only a brief outline of the model.

We consider a vertical hydraulic fracture of fixed height $H$ propagating along the $Ox$ axis due to the pressure of the fluid pumped into the fracture. We use a Cartesian system of coordinates such that $Oy$ is orthogonal to the fracture plane $Oxz$, and $Oz$ axis is directed upwards. The coordinates origin coincides with the location of the well. Following [9] we suppose that fracture aperture is constant along z-coordinate and vertical deformations are negligible. This implies, that we can limit ourselves to the plane strain approximation observing only the central cross-section $z = H/2$ of the fracture.

The reservoir is considered to be poroelastic meaning that it is represented as a two-phase continuum characterized by the displacement vector $\mathbf{u}$ of the elastic solid matrix (skeleton) and the pressure $p$ of the fluid within the pore space. The elastic response to the applied stress is assumed to be linear with the moduli $\lambda$ and $\mu$ as the skeleton's parameters. The filtration properties are characterized by the porosity $\phi$ and the permeability $k_r$. The speed $\mathbf{q}$ of the fluid flow in the porous medium is governed by the Darcy law $\mathbf{q} = -(k_r/\eta_r)\nabla p$ for a single-phase Newtonian fluid with the effective viscosity $\eta_r$.

Following [1, 6, 2] the mechanics of the poroelastic medium in quasi-static state is governed by the following system of equations:

$$\operatorname{div} \boldsymbol{\tau} = 0, \quad \boldsymbol{\tau} = \lambda \operatorname{div} \mathbf{u}\, \mathrm{I} + 2\mu\, \mathcal{E}(\mathbf{u}) - \alpha p\, \mathrm{I}, \tag{1}$$

$$S_\varepsilon \frac{\partial p}{\partial t} = \operatorname{div} \left( \frac{k_r}{\eta_r} \nabla p - \alpha \frac{\partial \mathbf{u}}{\partial t} \right), \tag{2}$$

where $\mathcal{E}(\mathbf{u})$ is the Cauchy's strain tensor $2\mathcal{E}(\mathbf{u})_{ij} = \partial u_i/\partial x_j + \partial u_j/\partial x_i$ $(i, j = 1, 2)$, I is the identity tensor, $\alpha$ is the Biot coefficient responsible for the solid-fluid coupling. The storativity $S_\varepsilon$ reflects the dependence of the Lagrangian porosity $\phi$ on $\epsilon = \operatorname{tr} \mathcal{E}$ and $p$ as in [5].

Symmetry of the problem with respect to $Ox$, $Oy$-axis makes it possible to solve equations (1)–(2) over domain $\Omega = \{(x, y) : 0 \leq x \leq R_x, 0 \leq y \leq R_y\}$ which cross-section is shown in Figure 1.

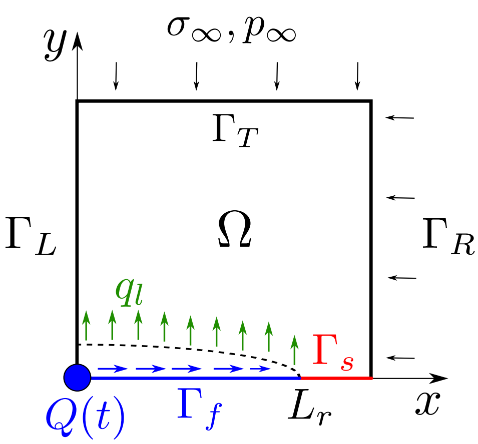


Рис. 1. The cross-section of the fracture by plane $z = H/2$

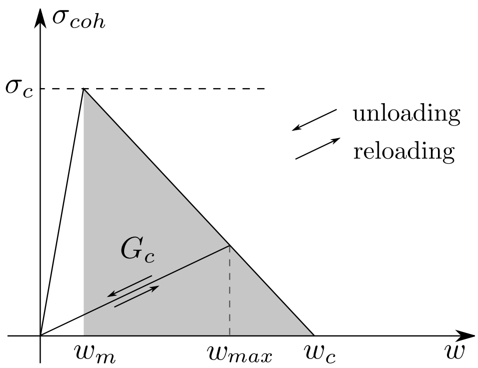


Рис. 2. Unloading/reloading relation ($G_c$ is the fracture energy, $\sigma_c$ is the critical cohesive stress value)

Over the right outer boundary $\Gamma_R = \{x = R_x; \quad 0 \leqslant y \leqslant R_y\}$ and the top outer boundary $\Gamma_T = \{0 \leqslant x \leqslant R_x; \quad y = R_y\}$, the confining far-field stress $\boldsymbol{\sigma}_\infty$ and the constant pore pressure $p = p_\infty$ are applied:

$$\Gamma_R,\ \Gamma_T : \quad p = p_\infty, \quad \boldsymbol{\tau}\langle \mathbf{n} \rangle = \boldsymbol{\sigma}_\infty, \quad (\boldsymbol{\tau}\langle \mathbf{n} \rangle)_i = \tau_{ij} n_j. \tag{3}$$

Henceforth, $\mathbf{n}$ and $\mathbf{s}$ denote the outer normal and tangential unit vectors to the boundary of the domain $\Omega$; the summation over the repeating index is implied. On the part of the boundary occupied by the fracture $\Gamma_f$ it is set the condition that the fracture propagates due to the pressure of fluid $p_f$ that is pumped into the fracture. The fluid flow inside the fracture is governed by the mass conservation law in the lubrication theory approximation, where the leak-off rate $q_\ell$ is proportional to the pressure $p$ gradient. Over the remaining boundary part $\Gamma_s = \{y = 0\} \setminus \Gamma_f$ and the left boundary $\Gamma_L$ the symmetry conditions hold. The lag between the fracture front and fluid front inside the fracture is neglected.

In order to model the fracture closure process, the cohesive zone model takes into account that the dissipation of the fracture energy is associated with unloading and reloading (see Figure 2) [8].

## 3. Numerical simulations

In this section a series of numerical experiments is described showing the sensitivity of the fracture geometry and fluid pressure to the reservoir physical properties: permeability and closure stress.

The following set of common input parameters are used. The computational domain is a square with a length of the side of $R = 45$ m. The physical parameters of the reservoir used in simulations are the Young's modulus $E = 17$ GPa, the Poisson's ratio $\nu = 0.2$, the initial porosity $\phi_0 = 0.2$, the Biot coefficient $\alpha = 0.75$. The initial pore pressure normalized to zero. Since we know $E$ and $\nu$, we can obtain moduli of elasticity $\lambda$ and $\mu$ by the known formulas. The storativity coefficient is defined as [5] $S_\varepsilon = (\phi_0 - \alpha_S)(1 - \alpha_S)/K$, where $K = \lambda + 2\mu/3$ is the bulk modulus.

The Newtonian viscous fluid (viscosity $\eta_f = \eta_r = 10^{-3}$ Pa $\cdot$ s) is injected into the fracture with the constant rate of $Q_0 = 4 \times 10^{-3}$ m$^2$/s for a period of 62.5 s before the pumping stops:

$$Q(t) = \begin{cases} Q_0, & 0 \leqslant t < 62.5 \text{ s}, \\ 0, & 62.5 \leqslant t \leqslant 100 \text{ s}. \end{cases}$$

The fluid filtrated from the fracture into the surrounding medium is assumed to have the same viscosity $\eta_r$ as the porous fluid Regarding the cohesive fracture parameters, the cohesive strength is set to $\sigma_c = 1.25$ MPa, and the cohesive force energy is taken to be $G_c = 120$ N/m.

3.1. **Influence of the permeability on the behavior of pressure decline curve.** At first, we analyze the sensitivity of the pressure decline curve to the permeability of the medium. We consider the following values of permeability: $k_r = k_0 \times 10^{-14}$ m$^2$, with $k_0 = 1$, 2.5, 5, and 7.5. The confining far-field stress $\sigma_\infty$ in all simulations is set to 7.2 MPa. The results of the simulations are presented in Figures 3, 4, 5.

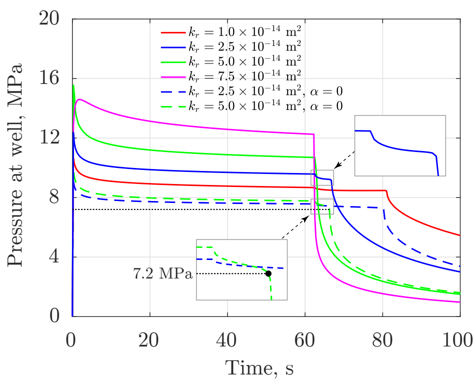


Рис. 3. Fluid pressure at wellbore for different permeability values in coupled ($\alpha = 0.75$) and uncoupled ($\alpha = 0$) cases

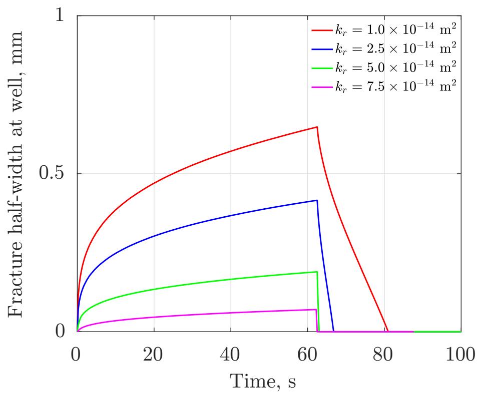


Рис. 4. Fracture half-width at wellbore for different permeability values (coupled case)

Figures 4, 5 show that the fracture propagates at longer distances for lower values of permeability. It can be explained using with the same argumentation as in [6]. Indeed, lower permeability leads to lower leak-off into the reservoir, and to lower extra closure stress imposed by the pore pressure action on the fracture walls. In

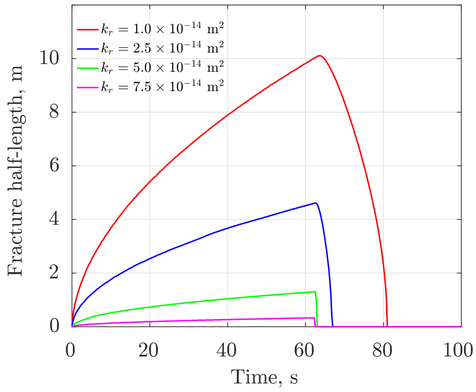


Рис. 5. Fracture half-length for different permeability values (coupled case)

turn, the lower leakoff leads to the longer fracture and higher borehole pressure at the higher values of permeability (see Figure 3).

Stoppage of the fluid injection results in a sudden drop of pressure at the wellbore. During the time interval from the moment of the stoppage to the fracture closure time, the pressure curve exhibits a distinctive “step”. One can estimate the permeability sensitivity by its length: a shorter “step” means higher permeability. Accordingly, one can propose an inverse problem of estimating the permeability by the size of the “step” under given other parameters of the medium.

It is worthwhile to mention that the numerical results indicate that the pressure curve is also significantly affected by the poroelastic effects. The contribution of the pore pressure (see Eqs. (1)–(2)) is determined by the Biot coefficient $\alpha$. Higher value of this parameter sets a strong connection between the pore pressure and the elastic stress, as well as between the processes of filtration and deformation of the medium [6]. For a non-zero Biot coefficient, the crack propagation is controlled by the deformation of the medium, as it affects the filtration. Meaningfully, one can observe the so-called “backstress” effect as an additional compression of the rock in the vicinity of the fracture caused by the pressure of the pore fluid filtrated into the reservoir [2, 7, 10]. The additional backstress leads to the increase of the pressure in the fracture at a given injection rate. In turn, such an increase causes a higher leak-off into the medium due to the filtration through fracture faces. The fluid efficiency goes down accordingly, and the size of the fracture decreases (see Figures 4, 5).

The described effect makes the fluid pressure at the moment of fracture closure be substantially different from the closure stress. Whereas, in standard algorithms for interpreting the pressure decline curve these values are assumed to coincide.

Conversely, for the Biot coefficient $\alpha = 0$, when poroelastic effects are disregarded, the pressure decline curves are represented by the dashed lines in Figure 3. In this case one can observe that the pressure of fracture closure is equal to the closure stress $\sigma_\infty = 7.2$ MPa shown in the enlarged fragment of Figure 3. Moreover, it can be noticed that the shape of the “step” depends on the influence of poroelastic effects: if $\alpha = 0$, it becomes longer because the pressure is lower, and the filtration and the closure process are consequently slower. One can make the following conclusion: even though the characteristic points (the stop of injection and the fracture closure) are distinguishable in both cases, although shifted in time, the results obtained within the poroelastic model allow the pressure decline curve to be interpreted more precisely, since the actual physical effects are properly taken into account.

3.2. **Influence of the closure stress on the behavior of pressure decline curve.** In this section we consider the behavior of the pressure decline curve for various values of the closure stress. From the curves in Figure 7 it is clear that the crack mouth opening displacement depends on the stress. In Figure 6 the pressure increases along with the stress, and we obtain a “step” again: the higher the stress, the shorter the “step”. This observation allows us to assess the relative value of the closure stress by the shape of the pressure decline curve. Also we note that in our model the fracture can continue propagating after the pumping stop. For example, it is clearly visible if the value of the closure stress is relatively low (see Figure 8, $\sigma_\infty = 1$ MPa).

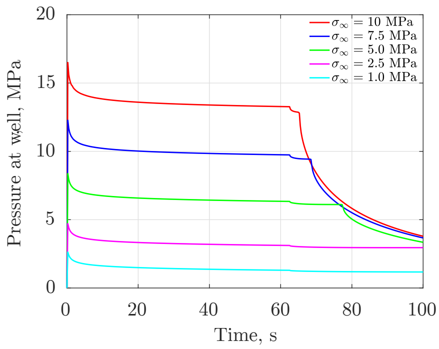


Рис. 6. Fluid pressure time history at wellbore for different closure stress values (coupled case)

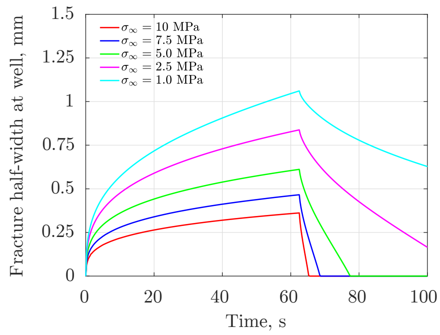


Рис. 7. Fracture half-width time history at wellbore for different closure stress values (coupled case)

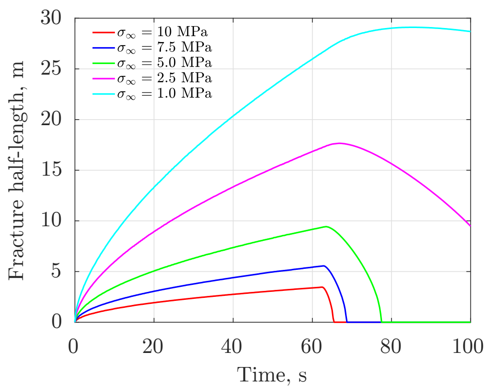


Рис. 8. Fracture half-length time history for different closure stress values (coupled case)

## 4. Conclusion

The mathematical model proposed in [2] is adapted to simulate pump-in/shut-in hydraulic fracturing schedules employed in mini-frac tests. A series of experiments regarding the poroelastic behavior of the rock medium was conducted in order to estimate the sensitivity of the computational results to reservoir parameters. The obtained wellbore pressure history and fracture geometries are analyzed relative to the permeability of the medium and closure stress. The characteristic features of the pressure decline curve are identified, and the influence of varying parameters is demonstrated. Particularly, the significant difference in pressure curve interpretation is observed in classical elastic and poroelastic cases. The performed analysis can be considered as a first step toward an accurate estimation of the pay zones parameters and better input data for hydraulic fracturing models.

## References

1. A.N. Baykin and S.V. Golovin, *Modelling of hydraulic fracture propagation in inhomogeneous poroelastic medium*, J. Phys.: Conf. Ser., **722** (2016), 012003.
2. A.N. Baykin and S.V. Golovin, *Application of the fully coupled planar 3d poroelastic hydraulic fracturing model to the analysis of the permeability contrast impact on fracture propagation*, Rock Mech.&Rock Eng., **51**:10 (2018), 3205–3217.
3. T.J. Boone, P.R. Kry, S. Bharatha, and J.M. Gronseth, *Poroelastic effects related to stress determ ination by micro-frac tests in permeable rock*, In J.-C. Roegiers, editor, The 32nd U.S. Symposium on Rock Mechanics (USRMS), 10–12 July, Norman, Oklahoma, 25–34, Norman, 1991, ARMA-91-025.
4. R.D. Carter, *Appendix i. derivation of the general equation for estimating the extent of the fractured area*, In G. C. Howard and C. R. Fast, editors, Drilling and Production Practice, chapter Appendix I, 267–268. Amer. Petrol. Inst., N.Y., 1957.
5. O. Coussy, *Poromechanics*, Chichester: John Wiley & Sons Ltd., 2004.
6. S.V. Golovin and A.N. Baykin. *Influence of pore pressure on the development of a hydraulic fracture in poroelastic medium*, Int. J. Rock Mech. Min. Sci., **108** (2018), 198–208.
7. Y. Kovalyshen, *Fluid-driven fracture in poroelastic medium.* PhD thesis, University of Minnesota, Minneapolis, 2010.
8. Kyoungsoo Park and Glaucio H. Paulino, *Computational implementation of the PPR potential-based cohesive model in ABAQUS: Educational perspective*, Engineering Fracture Mechanics, **93** (2012), 239–262.
9. V.V. Shelukhin, V.A. Baikov, S.V. Golovin, A.Y. Davletbaev, and V.N. Starovoitov, *Fractured water injection wells: Pressure transient analysis*, Int. J. Solids Struct., **51**:11 (2014), 2116–2122.
10. L. Vandamme and J. Roegiers, *Poroelasticity in hydraulic fracturing simulators*, JPT, **42**:9 (1990), 1199–1203.

Ekaterina Lgotina
Lavrenyev Institute of Hydrodynamics,
pr. Lavrentyeva, 15,
630090, Novosibirsk, Russia
Novosibirsk State University
1, Pirogova st.,
Novosibirsk, 630090, Russia
*E-mail address*: kate.lgotina@gmail.com

Alexey Baykin
Lavrenyev Institute of Hydrodynamics,
pr. Lavrentyeva, 15,
630090, Novosibirsk, Russia
Novosibirsk State University
1, Pirogova st.,
Novosibirsk, 630090, Russia
*E-mail address*: alexey.baykin@gmail.com

Sergey Golovin
Lavrenyev Institute of Hydrodynamics,
pr. Lavrentyeva, 15,
630090, Novosibirsk, Russia
Novosibirsk State University
1, Pirogova st.,
Novosibirsk, 630090, Russia
*E-mail address*: golovin@hydro.nsc.ru

Anton Krivtsov
Peter the Great St.Petersburg Polytechnic University,
29, Politekhnicheskaya st., Gidrotekhnicheskij korp. 1,
1, Gidrotekhnicheskij korp.,
Saint Petersburg, 195251, Russia